TECHNICAL UNIVERSITY OF LIBEREC
Faculty of Mechatronics, Informatics
and Interdisciplinary Studies

MIRROR ALIGNMENT CONTROL FOR COMPASS RICH-1 DETECTOR AT CERN

Doctoral Thesis Statement

Study programme: P2612 – Electrotechnology and informatics
Study branch: 2612V045 – Technical Cybernetics

Author: **Ing. Lukáš Steiger**
Supervisor: doc. RNDr. Miroslav Šulc, Ph.D.

Liberec 2013

Abstract

This Thesis summarizes various attitudes for the alignment measurements of large segmented mirrors. Especially in the field of Ring Imaging CHerenkov (RICH) detectors for particle physics, the measurement arrangement is limited mainly by the available space and material budget influencing the acceptance area of the spectrometer.

The detector RICH1 of the COMPASS experiment at CERN SPS is a large size gaseous Cherenkov detector with two reflecting spherical surfaces formed by hexagonal and pentagonal mirrors, with individual degrees of freedom for angular adjustment. The mirror elements must be very accurately aligned so to form a focused image in the detector photon detection area. Any misalignments distort the image and thus directly affect the detector resolution. The mirrors had been carefully adjusted before the start of the experiment data taking period, but the influence of external vibrations, temperature fluctuation and hydrostatic pressure in the radiator gas causes misalignments of some mirrors. There was no possibility to check and monitor this effect during the data taking period of typically $6-8$ months.

An original method was applied for on-line mirror alignment monitoring. The rectangular grid, placed near the focal plane of the mirror wall inside the detector vessel is illuminated by high luminosity LEDs. The image of the grid, reflected by the spherical mirrors, is monitored by digital camera. Small tilts of a mirror create discontinuities of the grid line image. The observed shift provides the direction and value of the mirror tilt. The required resolution of the measurement is in the order of 0.1 mrad.

Two attitudes, the relative measurement and the absolute measurement, are tested and compared with two independent methods. In the Thesis, image processing techniques are adopted to analyze the position of the grid image, deformed by a reflection on individual spherical mirrors. To determine the absolute misalignment of the mirrors the precise position of the camera has to be known. The position of the camera is calculated using the close range photogrammetry where the influence of optical system parameters has to be considered.

For the precise measurement of the mirror tilt a new method was developed based on the optical reconstruction of line images and photogrammetry targets positions. It is shown that the sensitivity of the monitoring method is sufficient, i.e. 0.1 mrad, and that the measured misalignments can be included in the particle identification algorithm. The positions of COMPASS RICH1 mirrors are determined.

Contents

1. Motivation and Goal of the Thesis

RICH counters allow to detect electrically charged particles. As the particle is traversing the medium of the detector it emits so called Cherenkov photons along its way through the detector. The resulted cone of light is then focused towards the photon detection area. The image focalization is obtained by a large reflecting (spherical) surfaces composed of many mirror segments of a smaller size, which must be very accurately aligned to form a single smooth reflecting surface. Any misalignment directly affects the detector resolution. The possibility to monitor and correct the misalignment of the mirror wall is difficult particularly in RICH detectors with extended gas radiators, where the mirror wall is placed inside the RICH vessel in the gas atmosphere. In such cases, the mirror wall alignment can be measured only before filling and closing the vessel of the detector. The goal of this Thesis is to enhance the resolution of the particle identification algorithm in Ring Imaging CHerenkov counters (RICH) using image processing methods for mirrors misalignments measurements.

In case of the COMPASS RICH1 detector the single photon angular resolution is about 2 mrad. The mirror misalignment errors contribute with the error of 0.6 mrad for the central region and 1.3 mrad in the peripheral region of the detection area of the RICH1 detector. To limit the mirror misalignments effect the continuous line alignment monitoring method (CLAM) was proposed. The desired resolution of the method should be 0.1 mrad. The aim of this Thesis is to apply the CLAM method to contribute to the increase of the angular resolution of the detector.

2. RICH1 detector

A Ring Imaging Cherenkov detector allows the identification of electrically charged subatomic particles through the detection of the Cherenkov radiation.

The COMPASS RICH1 [1] is designed to cover the acceptance of the first stage of the COMPASS spectrometer , achieving charge hadrons separation above three standard deviation levels (pions, kaons and protons) of particle momentum up to 60 GeV/c . Large volume vessel of the RICH1 detector is filled with heavy fluorocarbon radiator gas C_4F_{10} . Its refractive index is $n \approx 1.00153$ at 7 eV at atmospheric pressure and room temperature.

The ability of a RICH detector to successfully detect the particle depends on two principal factors: the effective angular resolution per photon σ and the maximum number of detected photons in the photon detection area. The number of detected photons depends upon the length of the particle path in the radiator, the photon transmission through the radiator material, the photon transmission through the optical system of the detector and the quantum efficiency of the photon detectors.

To produce sufficient number of Cherenkov photons in C_4F_{10} the overall length of the radiator vessel is of about 3 m. The volume is about 80 m^3. A dedicated control system is used to monitor and control gas pressure and temperature inside the vessel and it also maintains the radiator gas transparency.

Cherenkov photons emitted in the gas are reflected by two spherical mirror surfaces of total area larger than 21 m^2 towards the photon detection chambers. The chambers are placed outside the COMPASS spectrometer acceptance. Such arrangement focuses the cone of light produced by particle crossing the radiator towards the detector plane, where it generates image of a ring, regardless of the photon emission point along the trajectory of the particle.

The mirror wall is formed by a mosaic arrangement of 116 spherical UV mirror elements and is split in two parts by the horizontal plane on the beam

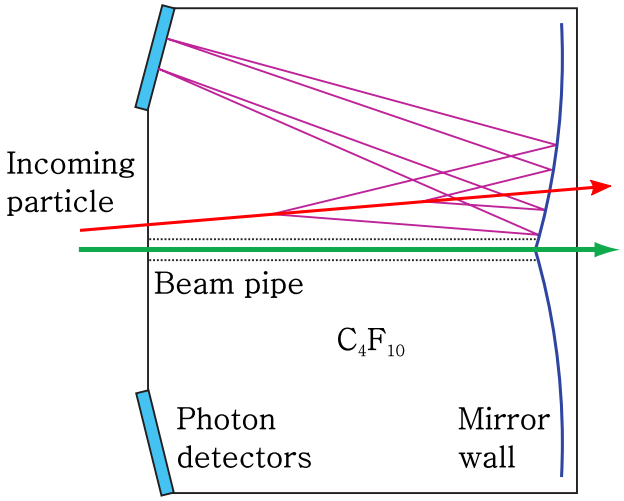

Figure 2.1: Working principle of the COMPASS RICH1 detector. Cherenkov photons emitted by the incoming particle in the radiator gas are reflected by two spherical mirror surfaces towards the photon detection chambers [3].

axis. The clearance left between adjacent mirror segments results in a 4 % loss of the reflecting surface. The radius of curvature of 6606 mm $\pm$ 20 mm is equal for both spheres [2]. To ensure a good reflectance in the VUV region ($83 - 87$ %), mirrors are coated with 80 nm reflective layer of aluminum (Al) and with 30 nm protective layer of magnesium fluoride (MgF_2). The mechanical structure supporting the mirror wall has a net-like configuration with spherical design made from aluminum. The mirrors are suspended to the nodal points . Due to this particular arrangement, only angular adjustment of the mirror units is possible.

The particle trajectory reconstruction and the dispersion that comes from the mirror imperfections and the mirror alignment errors contribute with the error of 0.6 mrad for the central region and 1.3 mrad in the peripheral region. Error in the mirrors alignment can be caused by initial installation and it can vary with temperature changes (material dilatation), pressure changes or mechanical vibrations. To eliminate the alignment error, and consequently to minimize the angular resolution of the RICH1 detector, it is suitable to monitor the alignment of individual mirrors and to set appropriate corrections. The overview of methods which are used to monitor the alignments of mirrors in RICH detectors is discussed in the next chapter.

3. State-of-the-Art of the mirror misalignment measurement

In the past several methods were developed for the measurement of the mirrors misalignments in RICH detectors. They have some limitations in the case of usage in the COMSPASS RICH1. As it was mentioned in the previous Chapter, the misalignment of mirror elements of the detector significantly affects the detector resolution. The mirror elements must be very accurately aligned to form a single smooth reflecting surface.

In the case of the alignment of the optical system with data collected by the spectrometer [4] alignment of the reference mirror has to be known precisely in advance. Moreover, a large statistics is needed, hence the information is averaged over a long time intervals. In case of COMPASS RICH-1 detector, not more than about one quarter of the mirrors, those, which are placed in the most populated areas, can be monitored with this approach.

The laser alignment monitoring system (LAMS) [5] can be adopted to ensure correct alignment of the reference mirror. Because of large number of components needed by the LAMS, the method can be used to monitor only a few mirror segments.

The main disadvantage of the most advanced method - surveying the mirrors with the theodolite [6] - is the need of direct access to the mirror setup. Thus, the surveying can be performed only when the spectrometer is not in operation mode.

In 2001, the initial alignment of the whole mirror wall of the RICH1 was performed and then remeasured using the autocollimation technique . Later, the alignment of selected mirrors was measured several times between the experiment data taking periods, typically once per year. Misalignments with a random distribution in the range of $0-1.5$ mrad used to be observed. The origin of the misalignments detected after the initial alignment procedure is not known yet.

4. CLAM - Online mirror alignment monitoring method

It was mentioned in the previous Chapter, that the monitoring of alignment of mirror walls in Cherenkov detectors for particle physics is performed mainly offline or in a long-time scale or for selected mirrors only. Almost realtime monitoring for all the mirrors of the mirror wall is not implemented so far. The first proposal of the on-line monitoring method, named Continuous Line Alignment Monitoring method for RICH mirrors (CLAM), was written by Sergio Costa and Jean-Christophe Gayde in 2005 [7]. According to feasibility study which was performed afterward, the production of a prototype started. In 2007 hardware parts of the CLAM were installed in the COMPASS experiment in the RICH1 detector.

Hardware arrangement

The mirror wall of the RICH1 detector forms a part of a sphere with known radius. The idea behind the CLAM method is as follows: If adjacent mirror segments are not coherently aligned, the image of an object reflected by these mirrors appears broken, not consistent. Thus, any discontinuity in the image of a rectangular grid of continuous lines corresponds to a relative mirrors misalignment.

The basic hardware components include four digital cameras for the monitoring of four different segments of the mirror wall, a regular grid of retro-reflective strips and two LEDs for each camera. All the parts of the system were properly chosen to meet the required resolution of mirror misalignment of 0.1 mrad.

In the arrangement, designed for the CLAM system, the retro-reflective strips of the width of 10 mm form a square grid with pitch of 100 mm. Circular photogrammetric reflective targets, each 10 mm in diameter, are

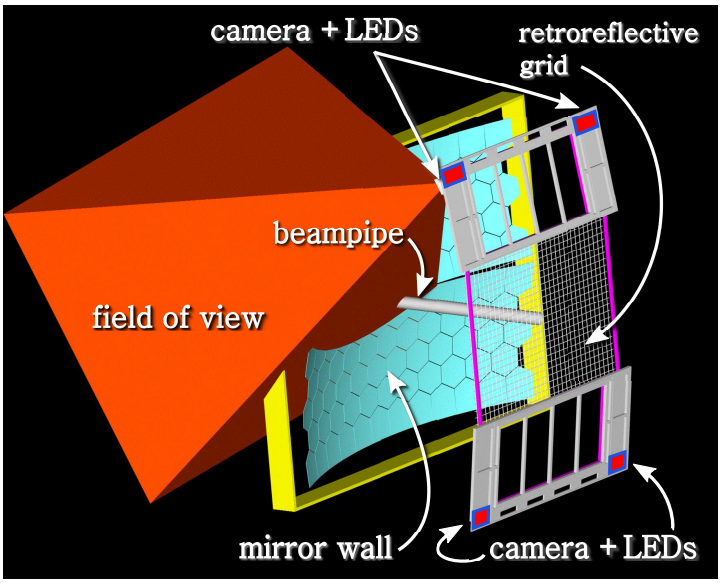

Figure 4.1: The arrangement of CLAM hardware components inside the RICH1 detector.

placed on the strips intersections. To avoid mechanical deformations of the grid, the grid is glued to an aluminum (Al) support. The grid is fixed only at the top and the bottom part and it is not stabilized in the middle part, a movement towards the mirror-wall may occur.

The retro-reflective grid is illuminated by high luminosity light emitting diodes (LED) LUXEON-LLXHL-LW6C 5500K HEXAGON produced by Lumileds [8]. A set of two LEDs is placed close to each camera, specifically, they are mounted in the camera holder.

The output of data collection can be seen in Figure 4.2. For the sake of clarity the picture colors are inverted. The picture was taken by Jura-Top camera. Some features of the CLAM can be seen on the photograph. The photogrammetry targets are mounted on the mirror wall frame. They are used to calculate the position of the camera. Shift of the grid lines in the mirror is shown in detail. Size of the shift indicates the mirror misalignment.

Mirror Misalignment Measurement

Two approaches are considered when one needs to evaluate mirrors misalignments - *relative* and *absolute measurement*. During the *relative measure-*

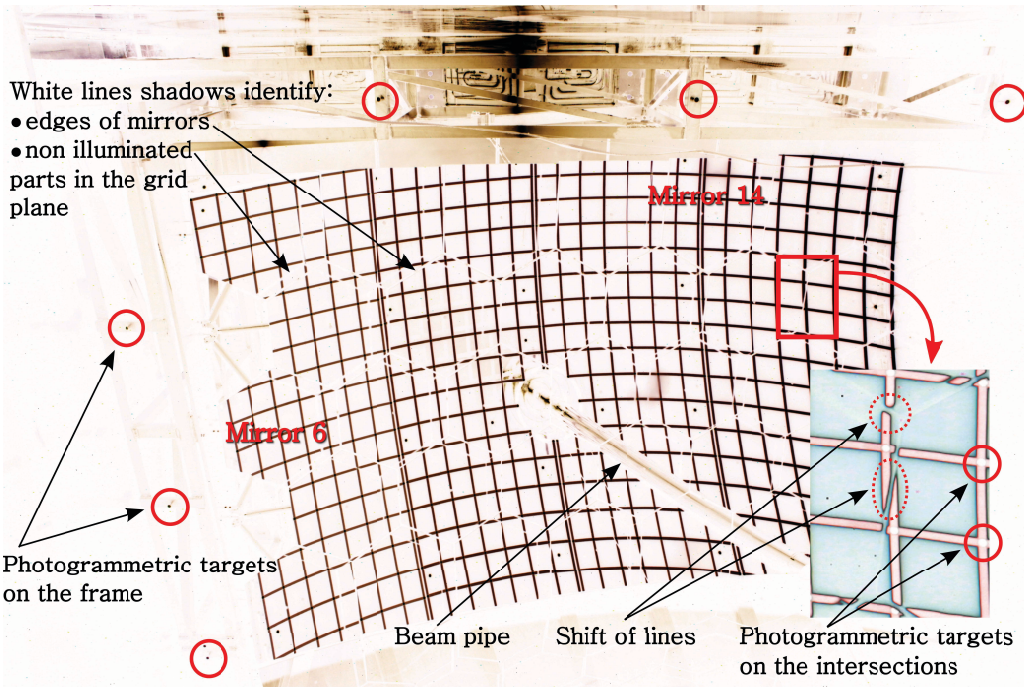

Figure 4.2: Example of a picture collected by one of the CLAM camera. To calculate the position of the camera, seven photogrammetric targets on the mirror wall frame are used. Every mirror is labeled. In detail, shift of grid lines is shown indicating the mirrors rotation.

ment, the positions of the grid lines reflected by the mirrors are evaluated from images taken at different times. The first image serves as a reference. Then, the other images are subtracted from the reference one. Consequently the change of mirror rotation is indicated in the subtracted image by arised line. Eventually, one could compare each mirror with its neighboring mirrors using just one picture. This would work on the assumption that surrounding mirrors are perfectly aligned. Unfortunately, several mirrors were misaligned since the beginning when the CLAM data collection started.

The position of the mirror wall is given by its center of curvature. If all the mirrors are aligned, all their centers of curvature would be focused in the same point, i.e. the center of curvature of the whole mirror wall. The so called *absolute measurement* method is aimed at the measurement and calculation of the center of curvature of each mirror segment of the RICH1 mirror wall.

5. CLAM - Relative measurement

The regular retro-reflective grid is reflected off the mirror wall and on the account, that the mirrors are spherical, the reflection image of the lines taken by the camera will be an image with the conic sections instead of the straight lines. Then, the mirror misalignment is detected as a discontinuity of conics. In the CLAM proposal described in the previous Chapter, authors suggest to measure the shift as difference of two images taken at different dates and times.

Calibration of the method

In laboratory conditions, an activity to find a relationship between the shift of conics in the image in horizontal and vertical directions, *hor* and *ver*, and the two angles, φ and θ, was performed for each single mirror position. The exercises were the main part of the diploma thesis by Marek Švec [9]. During the laboratory testing Marek Švec checked all the 30 possibilities of the relative mirror-camera positions of a RICH1 Jura-Top quadrant. The other quadrants (JB, SB, ST) are symmetric with respect to the JT quadrant.

The laboratory testing set-up was arranged as follows: A laser interferometer was used as a reference measurement instrument. A movable Canon camera holder was mounted in the plane of a rigid frame. Two LED light sources were connected with the camera holder. The retro-reflective grid was placed at the same relative position with respect to the mirror and the camera positions, as it is in the RICH1 vessel. An original COMPASS RICH1 spare mirror was mounted onto a stable holder, which can rotate around 2 axes.

Summary and results

During the relative measurement, the positions of the grid lines reflected by the mirrors are evaluated from images taken at different times. The first image serves as a reference. Then, the other images are subtracted from the reference one. It is obvious, that light conditions and camera settings have to be identical for the photographs that are about to be compared. Consequently, the change of mirror rotation is indicated in the subtracted image by arised lines.

In laboratory conditions the calibration parameters for every mirror of the mirror wall were obtained. It was computed , that depending on the mirror position within the mirror wall, the shift of one pixel corresponds to the mirror rotation of $0.14 \div 0.20$ mrad.

The relative measurement in the RICH1 was performed at different times in 2007: Before the start and during the COMPASS data taking period, which took six months, At changing pressure conditions, ranging from 957 to 968 hPa, At changing temperature conditions, from 21°C to 30°C). The comparison of the taken pictures shows that some mirrors exhibit a slow continuous motion, characterized by a typical tilt of 0.05 mrad in the horizontal and 0.11 mrad in the vertical directions. Some mirrors tend to be in a stable position after 2 months of the run.

In the relative measurement, the possible camera movements had to be considered. Several photogrammetric targets are fixed onto the peripheral frame of the mirror wall supporting structure. In the hypothesis, that the position of the frame is stable, the shift of the photogrammetric targets in the image indicates movement of the camera. The positions of the target centers were calculated by the circular Hough transform based on the gradient field of an greyscale image with resolution better than 0.5 pixels. The movement of the camera is apparent in the images which were taken before and after filling the vessel of the RICH1 detector with the C_4F_{10}. A horizontal movement of the target centers of about 2 pixels was observed, whereas the vertical shift was almost negligible. This indicates that the cameras have been slightly rotated of about 0.6 mrad due to the pressure change. After the RICH1 was filled, the camera position seemed to be stable within the range of the experimental uncertainty (0.25 pixel corresponds to a tilt of 0.035 mrad).

6. CLAM - Absolute method

In the previous Chapter, the relative measurement was described. It was emphasized that it is possible to measure displacements of mirrors in comparison to a reference picture which defines a reference set of mirrors positions values. On the other hand, the aim of the absolute measurement method is to determine directly the mirror tilt/orientation using only one picture. Every mirror segment is originally defined by its ideal position and its orientation according to the center of curvature C_k of the top or the bottom part of the mirror wall. The coordinates of both centers are given in COMPASS coordinate system. The picture taken by the camera is a result of a projection of the measured scene (3D $\rightarrow$ 2D). In the absolute method, the mirror position and its orientation is estimated using only the image of the mirror taken by the camera.

6.1 Photogrammetry

The process to obtain a relationship between the image coordinates and the real world coordinates can be divided into two basic steps: Interior orientation of the camera which provides the camera calibration and the exterior orientation of the camera which provides the position of the camera.

6.1.1 Interior orientation of a camera

A camera can be modelled as a spatial system with its perspective center. The model consists of a planar imaging area (CMOS sensor) and lens. The interior orientation parameters are the principal point, the principal distance and the parameters of functions describing imaging errors.

The imaging errors represent aberrations and distortions of the ideal central perspective model. Contrary to optical aberrations that affect radiometric quality of the final image, optical distortions affect the geometric

quality of the final image. The effect of radial-symmetric distortion and decentering lens distortion are considered in the algorithm of the absolute measurement.

Typically, the correction values are obtained by the self-calibrating bundle adjustment method. In our case, a plate with circular photogrammetry targets placed in well defined regular positions is used. The plate is photographed by the camera from several positions.

It has to be mentioned, that the CLAM cameras are placed outside the RICH1 detector. That means, that the light ray has to go through multiple media. First, the cameras are separated from the inner environment inside the detector by 1 cm thick glass planparallel window. Second, the cameras are placed in air atmosphere, while the RICH1 is filled with the C_4F_{10}, eventually with nitrogen.

Generally, before RICH1 is filled with C_4F_{10} ($n = 1.00131$) it contains only nitrogen ($n = 1.0002793$). In out-of-run periods of the COMPASS spectrometer, the RICH1 vessel is filled with air ($n = 1.0002724$). The stated values of the refractive indices, which can be found in [10], are valid for wavelength $\lambda = 546.1$ nm and for normal working conditions of the RICH1 detector, i.e. temperature $t = 25°$ C and atmospheric pressure $p_a = 101325$ Pa. Water vapor and oxygen traces are kept below 5 ppm [11]. The change of the gas from air or nitrogen to C_4F_{10} results in maximum radial shift at the edge of the sensor of about 0.0277 mm. Size of the pixel of the image sensor is 0.0082 mm [12], thus the radial shift corresponds to $0.0277/0.0082 \approx 3.4$ pixels.

Generally, the refractive index of a gaseous radiator depends on many parameters, mainly on the purity of the gas itself, the atmospheric pressure and the local temperature. Therefore, the value of refractive index is time dependent. Thanks to the gas circulation system of the RICH1, that was installed in July 2009, the inner gas environment of the detector is kept homogeneous. The rate of the circulation is in order of 20 m^3/hour [13]. However, the influence of the outer environment should be considered. For the purpose to which extent the environmental phenomena influence the refractive index, the finite element method model was developed and is discussed in the next Section.

First, in order to see the influence of the filling of the vessel with the C_4F_{10} it is convenient to develop a realistic 2-dimensional two-phase fluid flow FEM model which would be robust enough to see the changing density of the gas in time . Second, in order to see the changing density of the gas due to the influence of varying temperature around the vessel during the

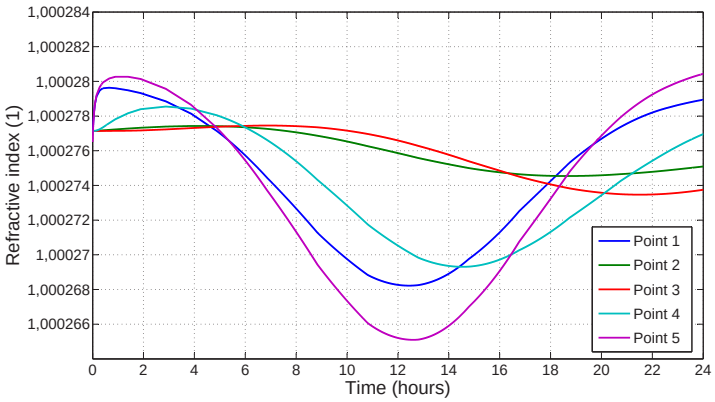

Figure 6.1: Change of the refractive index in the course of time. The values of n were determined in five selected points . It is obvious that the change of the temperature during the whole day in the range of ΔT does not tremendously affect the value of the refractive index.

day a FEM model using the heat transfer in liquids is developed .

The problems were solved using COMSOL Multiphysics software [14]. The solution primarily yields spatial distributions of the fluid velocity vector, the pressure and the level set function. Secondarily, it yields the total fluid density. The refractive index of the fluid directly depends on the density value.

The density of the gas inside the vessel can be changed not only during the filling but due to the change of ambient temperature or pressure. Here, the example of the FEM model of varying temperature in the course of one day is presented.

The change of the refractive index in the course of time can be seen in Figure 6.1. It is obvious that the change of the temperature during the whole day in the range of ΔT does not tremendously affect the value of the refractive index. The maximum change of the refractive index ($1.00026 \rightarrow 1.00028$) results in maximum radial shift at the edge of the sensor of about 0.0005 mm . Thus the radial shift corresponds to 0.065 pixels.

6.1.2 Exterior orientation of a camera and collinearity equations

The exterior orientation of a camera defines its location $[X_0, Y_0, Z_0]$ in space and its view direction $[\alpha, \beta, \gamma]$. The viewing directions form the orthogonal

rotation matrix $\mathbf{R} = \mathbf{R}_\gamma \mathbf{R}_\beta \mathbf{R}_\alpha$ which corresponds to the rotation about fixed axes in the order α, β, γ.

To calculate the position of CLAM cameras, 26 target points were installed on the mirror wall frame. Corrected image coordinates, obtained using the inclusion of interior parameters $[x', y', z']$, can be expressed as follow:

$$x' = x'_0 + \Delta x' - z' \frac{r_{11}(X - X_0) + r_{21}(Y - Y_0) + r_{31}(Z - Z_0)}{r_{13}(X - X_0) + r_{23}(Y - Y_0) + r_{33}(Z - Z_0)} \tag{6.1}$$
$$y' = y'_0 + \Delta y' - z' \frac{r_{12}(X - X_0) + r_{22}(Y - Y_0) + r_{32}(Z - Z_0)}{r_{13}(X - X_0) + r_{23}(Y - Y_0) + r_{33}(Z - Z_0)}$$

, where $[X, Y, Z]$ stands for coordinates of the corresponding object point. One can see, that Eq. (6.1) describes the transformation of the object coordinates into the corresponding image coordinates as functions of interior orientation parameters and exterior orientation parameters of the image.

A method to calculate the exterior orientation of a single image is called *space resection*. The method provides a non-linear solution. Due to the group τ of six dependent variables $\tau = \tau(X_0, Y_0, Z_0, \alpha, \beta, \gamma)$ at least three independent reference points in the object space (3D) are required to find a solution. Every point contributes with a set of two nonlinear equations.

Correct solution of the least-squares adjustment can be found only when a good initial guess of the τ is provided into the procedure. Approximate values for the first step of the algorithm were obtained by the direct measurement of the RICH1 detector from the CAD drawings [15] and by the simulation of the CLAM system in MATLAB environment.

Image processing

Photogrammetric targets are equally distributed on the mirror wall frame of the supporting structure. They are coplanar and when one looks at the CLAM pictures it can be seen that they are placed at the edges of images. Consequently, the correction parameters (Sec. 6.1.1) are non-negligible according to the position of the reflection points on the mirror wall. It also means that the illumination of the targets differs significantly. Furthermore, during the images taking, it happened that only one of the two diodes was working. In such cases, the illumination changed completely. As a result, some of the mirror-wall photogrammetric targets were not illuminated and therefore, the number of inputs to the space resection algorithm decreased. The following image processing techniques were chosen and as well their

adaptation was adjusted to suppress such variations in the input to the camera position algorithm.

When looking for the positions of the mirror wall photogrammetric targets in an image, k-means clustering method [16] is the core of the algorithm. Image preprocessing techniques used in the program eliminate most of spurious objects in the image. Photogrammetric targets are the most illuminated parts of the image, hence it is possible to threshold the image. Of course, the light intensity varies across the illuminated area. The threshold value is estimated automatically using the Otsu's method [17]. According to the estimated value the threshold is overwritten. There are two values of thresholds to be used. They correspond to the intensity values of the investigated targets. The values were chosen experimentally. As a result of the thresholding, a binary image is obtained and connected components can be found. In some cases tha area of the components is too large (expected diameter of the target is $3 - 9$ pixels). It happens when the light intensity is too high, or there are significant reflections in the image . Consequently, the procedure has to be repeated with increased threshold. During the preprocessing too small components are also deleted. Finally, only one or no component is left in the image. In case of purely illuminated targets, number of components is equal to zero and the threshold has to be decreased. In case that only one LED is switched on during taking photographs, some target may not even be visible in the picture. Very low threshold value can help, unfortunately many spurious objects arise as well. In such case the morphological opening can be applied with properly defined structuring element in the shape of disc.

6.1.3 Sensitivity analysis of the camera position algorithm

The sensitivity analysis is the study how the uncertainty in the input to the mathematical model influences the final result, specifically the camera position. Several tests have been performed to ensure the stability of the algorithm.

First, the camera position was computed hundred times to verify algorithm repeatability. Input to the algorithm was kept identical. Two variants were tested: (i) The targets pixel coordinates were calculated once and (ii) The targets pixel were calculated anew at every repetition. The result was identical. The standard deviation of the repetitions was practically zero which means, that the the camera position algorithm gives equal results for

invariable input.

In the previous Chapter, measured position of the photogrammetric targets placed on the mirror wall frame was discussed. To show the importance of accurate values of the position coordinates of the targets and the influence of the target coordinates on the camera position determination, the input coordinates (given in 3D) of selected targets were shifted ± 10 mm. The inaccuracy of the camera position determination for the photogrammetric target TH1 is shown in Figure 6.2. For every photogrammetric target a set of three subtests was performed, where for each test only one coordinate varies. The effect is calculated for each coordinate of the camera position.

To evaluate the positions of all CLAM cameras, the maximum of seven photogrammetric targets for each camera can be used. Furthermore, all the targets are coplanar and placed at two borders of the image. The task of the following test is to identify the minimum number of photogrammetric targets as inputs. It can be shown that the position of the selected camera is set correctly with minimum of four targets. The procedure was performed as follows: There are seven targets in total. Every run of the algorithm, the input data of one target are removed from the algorithm and the position of the camera is calculated. The procedure continues until only one target is left in the input data. Analogously, the influence of only one missing target out of seven was tested. Every run of the algorithm, only one target (out of seven) is removed. The more distant target from the camera, the largest is the effect on the accuracy of the camera position coordinates determination.

The last test shows an influence of the time of illumination of the mirror wall, together with the effect of the left or right diode switched off. The time of illumination ranges from 0.5 to 5 seconds. The measurement was repeated again with changed shutter setting of the camera from 3.2 to 6 seconds. The main source of error is caused by the switched off diode placed on the right side of the camera. In such conditions, target TH3 is not illuminated. The effect is apparent especially for low illumination times (standard deviation is about 8 mm). The algorithm works reasonably well when both LEDs are switched on, or even left LED only (standard deviation is about 0.3 mm). According to the camera position computations, the optimal LED illumination time is about $3 - 4$ seconds, the exposition time is not the crucial parameter.

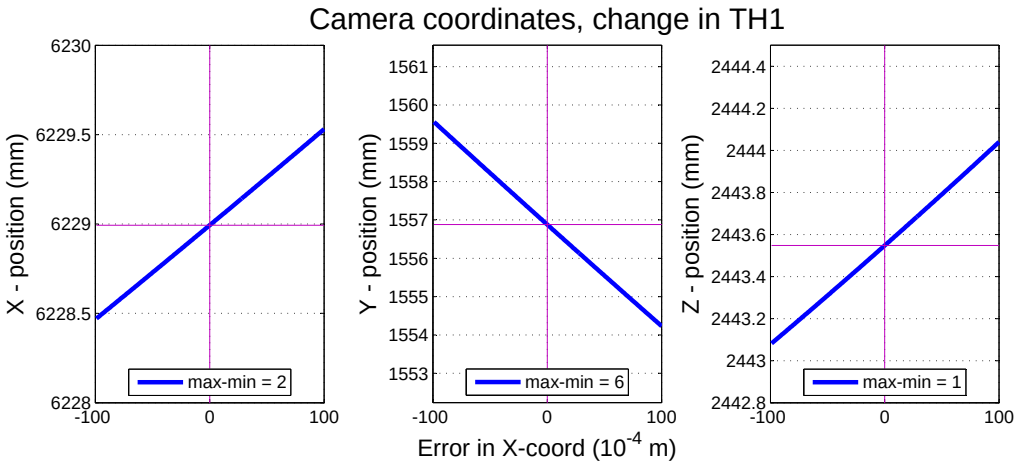

(a)

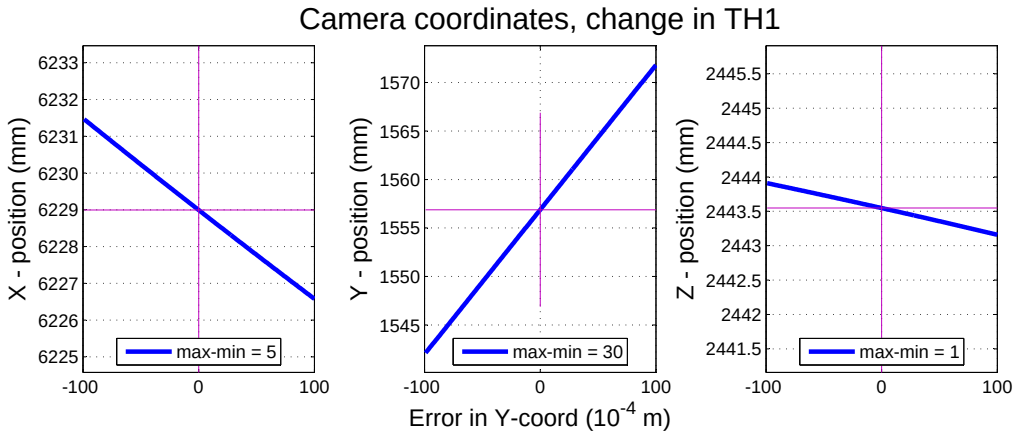

(b)

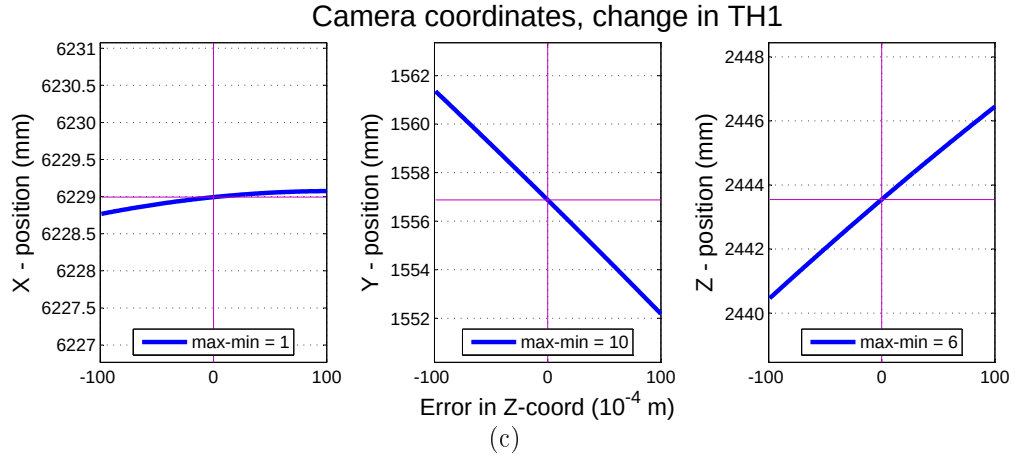

(c)

Figure 6.2: Camera position determination - inaccuracy in TH1 target coordinates was simulated. For every photogrammetric target a set of three subtests was performed, where for each test only one coordinate varies. It can be seen the influence for each coordinate of camera position.

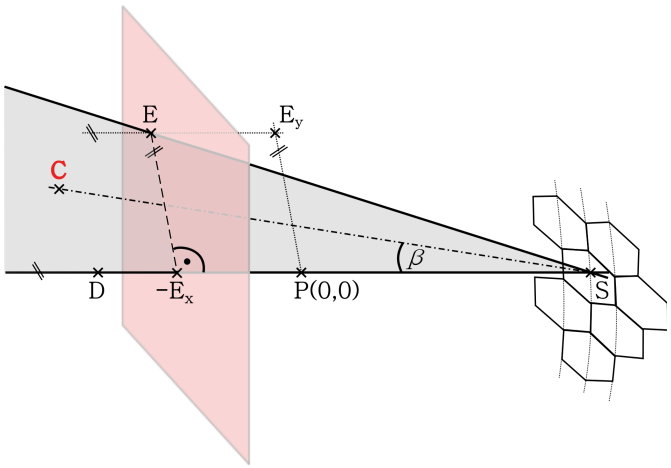

Figure 6.3: Determination of mirror orientation - 3D scheme of the geometry used in the algorithm for the absolute measurements of mirrors misalignments. P is the principal point of CLAM camera, E is point of the retroreflective rectangular grid and D is the image of the point E on the camera sensor, S stands for the reflection point on the mirror surface and C for the center of curvature of the mirror.

6.2 Determination of mirror orientation

The final step of absolute measurement method is to determine the misalignments of individual mirrors of the RICH1 mirror wall. In the Thesis, the algorithm, based on ray optics, is invented. Every mirror is equipped with a joint which allows it to rotate around two orthogonal axes. Its position can be adjusted with angular resolution $\Delta\alpha = 2.5$ mrad/turn with no hysteresis (Sec. 2). Well aligned mirrors share the same center of curvature. The center of curvature C_k for top and bottom part of the mirror-wall are different, but for the sake of generality we will use only C. The coordinate system is defined by the COMPASS survey coordinate system.

The idea behind the algorithm of finding the misalignments is simple. It assumes that the position of the center of curvature of a mirror changes with the mirror misalignment. The principle of the algorithm is shown in Figure 6.3. P is the principal point of CLAM camera, E is point of the retroreflective rectangular grid and D is the image of the point E on the camera sensor. The positions of points P and D were calculated in previous Section (Sec. 6.1). The position of E was measured with the precision of 0.5 mm in every coordinate. The reflection point S on the mirror surface

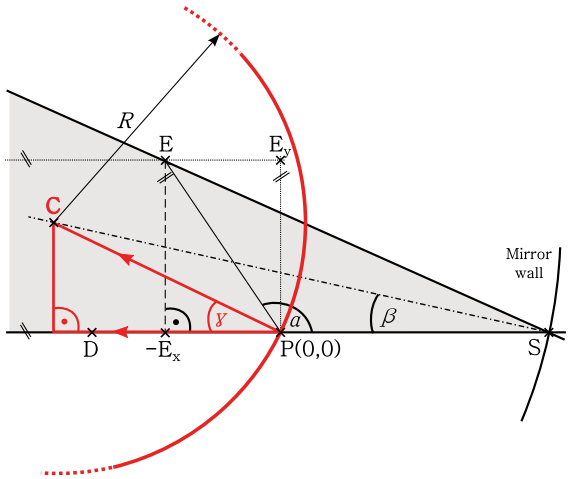

Figure 6.4: Determination of mirror orientation - principle geometry in 2D coordinate system defined using the positions of the points P, E, D. P is the principal point of CLAM camera. It defines the origin of the system. E is the point of the retroreflective rectangular grid with the axes projections E_x and E_y into the 2D plane. The point D is the image of the point E on the camera sensor, S stands for the reflection point on the mirror surface and C for the center of curvature of the mirror.

is not known while only the *ideal* center of curvature C_{id} is known. Also, the ideal the radius of curvature R_{id} of the spherical mirror is known. We search for the centers of curvature C of individual mirrors.

Since points P, E, D are theoretically coplanar, it is possible to define 2D rectangular coordinate system (Fig. 6.4), where the origin is set in the point P, i.e. $P = (0, 0)$, and the x-axis is defined by the direction of the vector $\vec{DP}$. E_x and E_y are 2D coordinates of the point E. According to the given geometric system, $S = (u, 0)$, where $u = \left|\vec{PS}\right|$. Then, C can be expressed as:

$$C = \vec{PS} + \vec{SC} = (u, 0) + (-R\cos\beta, R\sin\beta), \tag{6.2}$$

where β stands for the reflection angle of the mirror surface. There are two unknown variables, u and β. Using the law of sines, the position of the point C in 2D can be estimated using the equation:

$$C_{2D} = \left(\frac{|PE|\sin(\alpha)\cos(2\beta)}{\sin(2\beta)} + |PE|\cos(\alpha) - R\cos(\beta), \quad R\sin(\beta)\right) \tag{6.3}$$

For a set of input points P, E, center of curvature C_{2D} is obtained as a function of parameter β. Back-projection of the C to 3D coordinate system can be resolved using following considerations:

$$(C - D) \cdot [(P - D) \times (E - P)] = 0 \tag{6.4a}$$

$$\left|\vec{SC}\right| - R = 0 \tag{6.4b}$$

$$\|C - P\| - \|C_{2D}\| = (C - P) \cdot (C - P) - \|C_{2D}\|^2 = 0 \tag{6.4c}$$

$$\frac{(C - P) \cdot (P - D)}{\|C_{2D}\| \, \|P - D\|} - \frac{C_{2D,x}}{\|C_{2D}\|} = 0 \tag{6.4d}$$

The meaning of Eqs. (6.4a) - (6.4d) is the following: Eq. (6.4a): Points D, P, E, C are coplanar, Eq. (6.4b): The distance between points S and C is equal to the radius of curvature of the mirror, Eq. (6.4c): The distance between the points P and C. In other words, it is the equation of a circle with the center in P, Eq. (6.4d): The angle γ are equal in 2D and 3D systems (Fig. 6.4).

The theoretical position of the center of curvature of every mirror is given in spherical coordinates R, φ, θ relative to the ideal center of curvature of the top/bottom sphere [18]. The coordinate system is defined according to Figure 6.5: The origin is at the sphere centre, the vertical z-axis is in the upwards direction, the x-axis lies on the vertical symmetry plane of the spheres and y-axis is perpendicular to the zx plane. xyz axes share directions with the COMPASS survey coordinate system. For spherical coordinates, the angle θ is measured from z-axis towards the polar vector while the angle φ is measured from x-axis towards the projection of the polar vector into the xy plane.

The absolute misalignments of the mirrors are given as differences of the spherical coordinates $\Delta\varphi, \Delta\theta$. The misalignment is computed from the ideal center of curvature of the sphere C_{id}, the calculated center of curvature C of selected mirror and the center of the mirror M_S. Spherical coordinates of the mirror center are recalculated according to the calculated center of curvature C. Finally, the misalignments are calculated by subtraction of the original spherical coordinates of the mirror center of the recalculated ones.

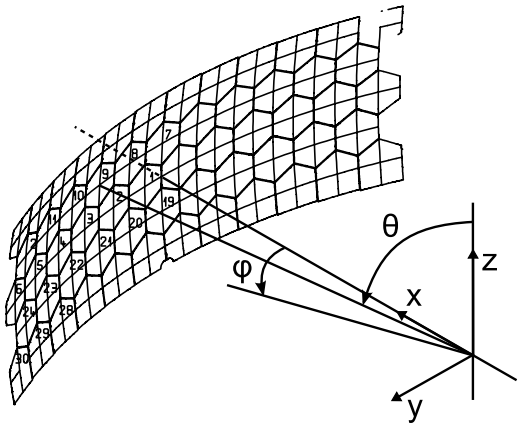

Figure 6.5: Determination of mirror orientation - The spherical coordinate system in the RICH1.

Image processing

The inputs to the algorithm of finding the mirrors misalignment are the position of CLAM camera P, 3D coordinates of the retroreflective rectangular grid point E, the ideal center of curvature of the sphere C_{id}, ideal position of the center of the mirror M_S and a picture taken by the camera.

In the algorithm, mirrors are evaluated separately, i.e. the image is cropped to contain only a selected mirror. Every mirror reflects part of the grid towards the camera, hence the grid of conics emerges in the picture. As it was discussed earlier, only the intersections of conics are used in the calculations. At the intersections, photogrammetric targets are glued . The first step of the algorithm is the determination of the targets positions in the image.

The targets are surrounded by dark border. From the perspective of image processing, the border is too narrow to be distinguished from the illuminated background which is formed of the stripes. Practically, the the border of the target is visible only for low times of illumination. Also, the circular targets appear in the image as ellipses. The idea to separate the targets from the grid is to apply the morphological image opening (Sec. **??**) with properly defined structuring element in the shape of line. The line structuring element is given by its length (in pixels) and by its angle (in degrees). At first, the inclination of lines of the grid has to be determined. The opening procedure is applied with angles from 5 to 180 degrees and the threshold value of the cropped image is computed. Maximum value of the

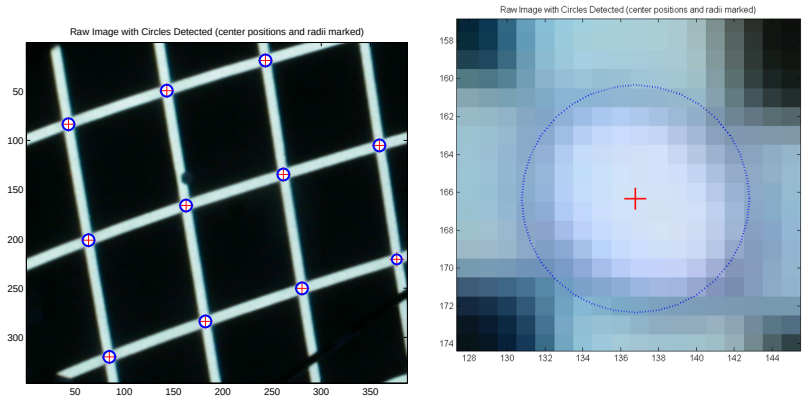

(a) (b)

Figure 6.6: Detected reflections of photogrammetric targets in the image, (a) for one mirror, (b) in detail. The centers and edges of circles are found and marked.

threshold corresponds to the angle between the lines in the grid image. The procedure is applied twice for the two directions of lines forming the grid. The opening procedure is reapplied with known angles in such a way that the resulted images contain only horizontal or vertical lines. The intersections are found using the logical operator AND of the two black-white images. As a result, approximate positions of the targets are found and it is possible to treat them separately. In every target region the connected components are found and evaluated in a way that only pixels forming the targets retain. The procedure is similar to the one applied in Sec. 6.1.2. The area of the target consists of pixels of different intensity values. The center position of the target is then given based on pixels locations and intensity values as it can be seen in Figure 6.6. Using Eq. (6.1) 3D coordinates of the centers D can be calculated.

The next task of the algorithm is to find the match between the points E and D. It was already explained, that all the points lie in the DPE plane. The reflection point S of a specific target on the mirror can be estimated from known coordinates of C_{id} and of the pair of points D, P. For every pair of points D, P a line is created. The intersection of the line and the circle with the center in C_{id} and the radius R gives us an estimation of the reflection point S. It is obvious that the angle of reflection β given by $\angle PSC_{id}$ and $\angle ESC_{id}$ should be similar. Both calculations are done and results are compared. Due to inaccuracies in estimated data a table of

possible angle matches is created. For every record in the table, the distance between C_{id} and the plane given by the points PSC_{id} is calculated. The least distance corresponds to the match between E and D.

Finally, the set of equations (Eq. 6.4) can be formed and evaluated to obtain the center of curvature of investigated mirror. There are four unknown variables in the set of equations: The coordinates of C and the angle of reflection β. The non-linear equations are solved using Gauss-Newton method, the initial parameters are set as C_{id} and $\angle PSC$ for each pair of points E, D.

6.3 Results

To prove the concept of the absolute measurement algorithm, simulations and laboratory tests were performed. Results of the algorithm applied on real data is also discussed.

6.3.1 Simulations

The simulations were performed to estimate the accuracy of the mirror position determination. In the simulations, the reversed order of the algorithm is applied. In the preparation phase, only the principal point of the camera P and the object points in the image D are used as inputs. Mirror misalignment angles are set artificially and consequently, the center of curvature C and the targets on the grid E are calculated. Then, the position of all the points is known and the algorithm may run as it was described in Sec. 6.2, with D, P, E, C_{id} as the inputs, to search the previously calculated C. The resulting error of the algorithm is less than 2 %.

6.3.2 Sensitivity of the absolute method algorithm

In Sec. 5 the laboratory measurement, performed in order to calibrate the CLAM method, was described. In the measurement, a relationship between the shift of conics in the image in horizontal and vertical directions, *hor* and *ver* (in pixels), and the mirror misalignment angles, ϕ and θ (in mrad), was found for each mirror. Mirrors were tilted gradually with the least step of 0.05 mrad. It can be shown that the CLAM method detects every step of the mirror tilt.

It should be noted, that the position of the grid used in the measurement does not entirely correspond to the grid used in the RICH1 detector.

Furthermore, the position of the camera is not known. Therefore, the test can be performed only with a few mirrors where predefined points E match points D which are detected in the image. Except this detail, the absolute algorithm is used as it would process the real data from the CLAM system in the RICH1 detector.

6.3.3 CLAM measurements in RICH1 detector

Now, the absolute algorithm is finally tested on real CLAM data, i.e. the pictures of the RICH1 vessel space which are taken by the CLAM cameras. The influences of the time of illumination and filling the RICH1 vessel with the C4F10 are discussed.

Time of illumination influence

The time of illumination of the mirror wall, together with the effect of left or right diode switched off, was tested. Distribution of the illumination intensity across the mirror wall is not homogeneous, it varies with the mirror relative position towards the source of illumination.

It emerged that the mirror misalignment variations are mainly correlated with the camera position estimation . Regardless of the considered number of LEDs used to illuminate the scene, the variations of the misalignment is less than 0.1 mrad. Considering only the case of both LEDs switched on, the variation is less than 0.05 mrad. Time of illumination of two LEDs ranges in the interval of $0.5 \div 4.0$ seconds.

Filling RICH1 vessel with C_4F_{10}

During the non-operational mode of the COMPASS experiment, the vessel of the RICH1 detector is filled with the air. Typically, before the start of COMPASS run period, the vessel is filled with the nitrogen and subsequently with the radiator gas C_4F_{10}. CLAM pictures were taken during filling of the vessel: Before the filling (100 % of nitrogen), during the filling (12, 46, 60 % of C_4F_{10}) and at the end of the filling (100 % of C_4F_{10}).

According to the FEM model , the density and by extension the refractive index of the gas is changing during the filling of the vessel. This effect was also proved using the absolute measurement algorithm , where only refractive index of the air is taken into account in the computations. The maximum change of the mirror misalignment at the level of 46 % of C_4F_{10} inside the vessel is correlated with the change of the calculated position of

the camera. From the FEM simulation results, it is known that the radiator gas fills the vessel gradually from bottom part of the vessel. Since the targets TJ4-TJ6 are inside the C_4F_{10} gas whereas the rest of the targets are still in the nitrogen atmosphere, the camera position is not calculated properly.

Measurements during COMPASS run

The mirror misalignments emerged during 2009 were evaluated. The measurements were randomly distributed over the COMPASS run period, i.e. between May and September 2009.

In 2001, the whole mirror wall was aligned and the measured residual misalignments showed a standard deviation of 0.06 mrad. The measurements of the misalignments were performed with the theodolite in autocollimation mode method . In following years, the mirrors alignments were measured several times between the experiment data taking periods (from 2002 to 2012 . Because of a certain difficulty of the theodolite measurement method, the time and space demands, only a few selected mirrors were investigated. The theodolite must be oriented to the center of mirror very precisely. Looking at several theodolite measurements in the RICH1 detector, an error in the theodolite position or an inclination of 1 cm corresponds up to 1.6 mrad error in the mirror misalignment estimation. During the theodolite measurements, the misalignments with a random distribution in the range of $0 - 1$ mrad have been observed, with a few elements exhibiting the misalignments of about 1.5 mrad. The cause of the misalignments emerged after the initial alignment is not known. When one compares the theodolite method with the applied CLAM method, the values differ significantly.

The detected misalignments of all the mirrors are shown in Figure 6.7. Only two mirrors are not measurable by the CLAM method in RICH1 detector, NB58 and NT48, because in the camera field of view the both mirrors are hidden behind an obstacle. The histograms in Figure 6.8 summarize the misalignments of the mirrors for the angles in horizontal and vertical direction, ϕ and θ. The resulting values indicate that almost 50 % of mirrors are horizontally misaligned up to 3 mrad at maximum and 65 % of mirrors are vertically misaligned of about 3 mrad at maximum.

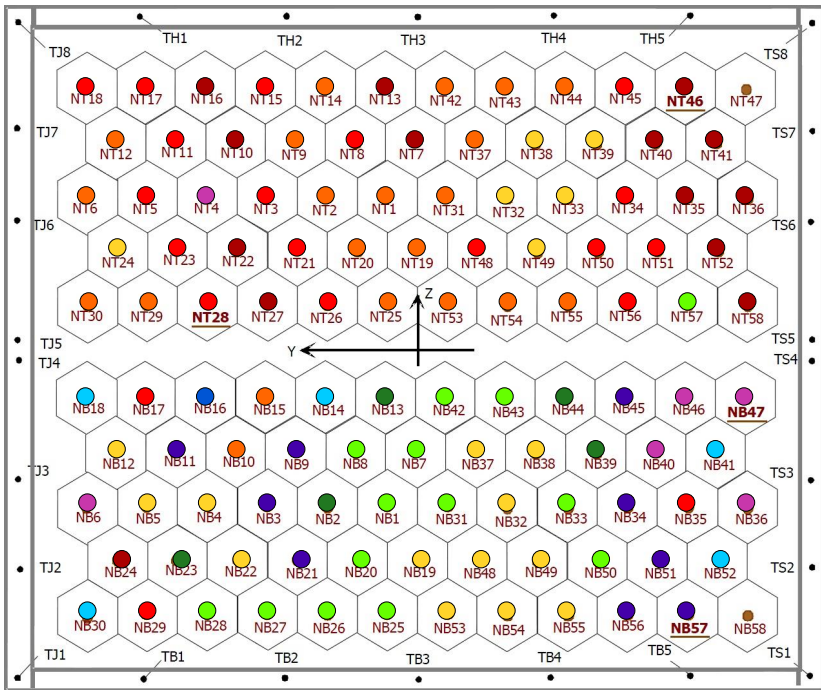

(a)

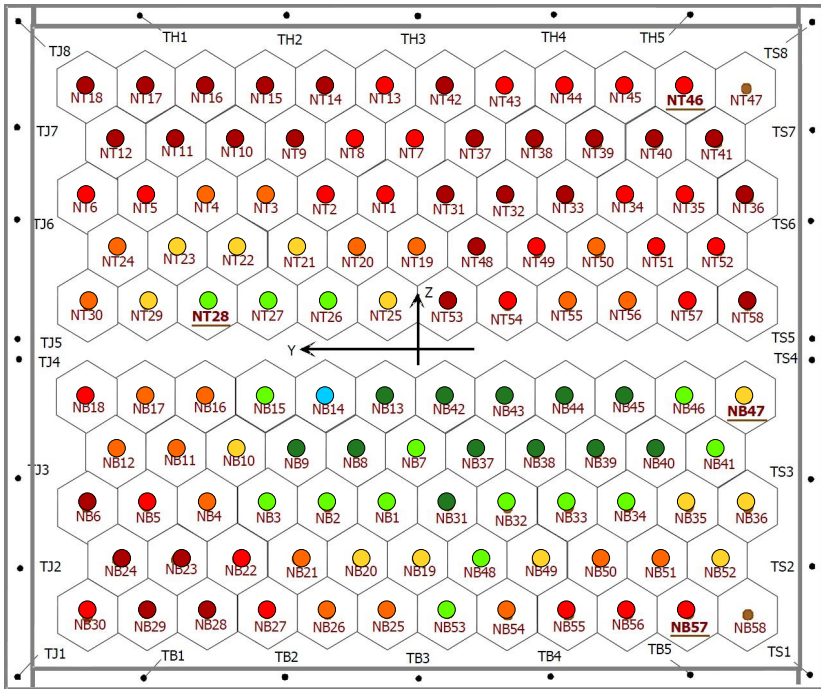

(b)

Figure 6.7: A complete list of detected mirrors mislignments (a) in the horizontal direction and (b) in the vertical direction. The colors correspond to the histograms values in Figure 6.8

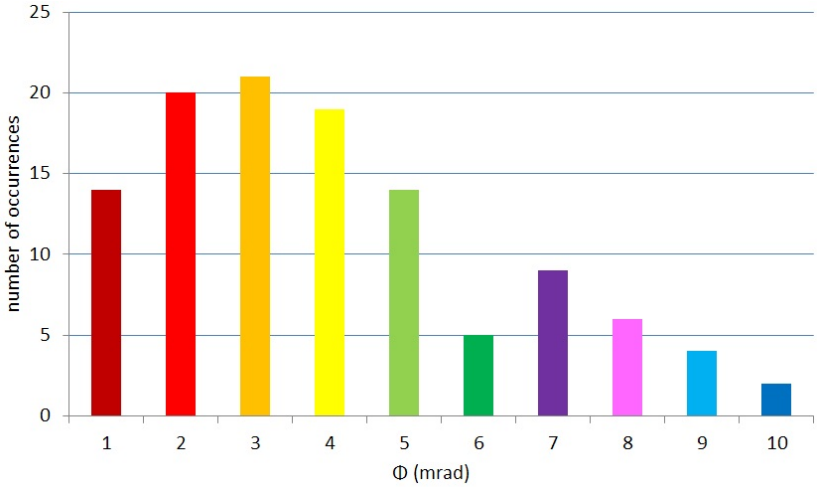

(a)

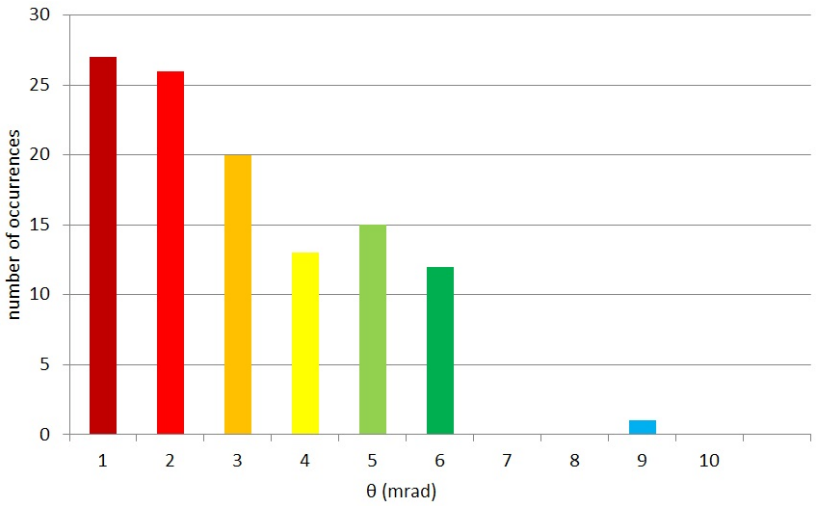

(b)

Figure 6.8: Histograms which summarize the detected misalignments of the mirrors. The resulting values indicate that almost 50 % of mirrors are horizontally misaligned up to 3 mrad at maximum and 65 % of mirrors are vertically misaligned of about 3 mrad at maximum.

6.4 Prospects

The Cherenkov photons originated in the RICH1 detector hit the reflective surface, the mirror wall, in a pseudo-circular region, i.e. the disk. The reflection point of each individual photon is not known because the photon emission point is randomly distributed along the particle path in the radiator (Sec. 2). The disk might be entirely included in a single mirror element or it can be shared among several adjacent mirror elements. Since the Cherenkov angle at saturation is 52 mrad, the disk can be shared by three mirrors at maximum. In case of any misalignment of the mirrors, parts of the image of the disk in the photon detection area are distorted. The detected photons do not follow the ring shape fluently and the particle identification algorithm might be misguided, especially in the case when more events are detected at the same time.

In the previous Chapters the ability of the CLAM method to detect mirrors misalignments was discussed and proved. There are two possible ways of prospective work to be followed: (i) to include the results of the CLAM measurements in the COMPASS data analysis or (ii) to directly correct the position of individual mirrors using the joints.

In the first case, the information about the mirror alignment can be used in the reconstruction and data analysis package for the RICH1 detector, called RICHONE [19].

In the second case, the corrections could be applied directly if the mirror wall is equipped by remotely driven actuators. The requirements of such a system, which would be able to apply such corrections, are the resolution of the applied positioning and the compatibility with the radiator gas purity, since the good UV-light transmission of the radiator gas down to 160 nm has to be preserved. Light piezo micro-metric actuators can adjust the individual mirror inclination; they are compatible with the radiator gas purity and they can be locally mounted without causing a significant increase of the mass of the overall radiation length of the mirror wall. Thus, the risk that an extra weight would deform the mirror suspension structure would be avoided.

The feasibility of the proposed application has been tested and proved in a laboratory exercise, using a RICH mirror element mounted on a holder identical to the RICH1 one. The mirror was tilted in the range of ± 6 mrad. Within the measurement resolution of 40 μrad, no hysteresis or nonlinearity were observed in the whole tested range [20].

7. Conclusions

The Thesis was focused on the study of possibilities to monitor the alignment of a large set of spherical mirrors which form the shape of a sphere. It was shown that the use of the CLAM digital photogrammetry based methods can offer an attractive approach to remotely measure the mirror misalignments with sufficient accuracy 0.1 mrad and speed comfort of the procedure.

In the field of particle physics, in RICH detectors with extended gas radiators, such as RICH1 of the COMPASS experiment at CERN SPS, image focusing is obtained by a large reflecting surfaces formed by mirror segments of a smaller size. The mirror walls are included in the gas vessel and they are sitting in the acceptance region of the experimental setup. The mirror segments must be very accurately aligned to form a single smooth reflecting surface. Any misalignments result in poorly focused images, directly affecting the detector resolution.

State-of-the-art methods of the mirror wall misalignment measurements are summarized.

Basic principles of the optical online monitoring system of the mirrors misalignments, the CLAM method, is introduced. The method was proposed by Sergio Costa and Jean-Christophe Gayde in 2005. The proposal was adopted in the RICH1 detector in 2007.

Two ways to measure the mirrors misalignments discussed in the Thesis: the relative and absolute measurement. The both methods were implemented by the author in the frame of this Thesis. The relative measurement is based on the comparison of pictures taken by the camera. It measures a difference of the taken picture with the reference picture. A laboratory measurement was performed to obtain the relationship between the shift of conics in the image in horizontal and vertical directions and the corresponding inclinations for each mirror.

The new absolute measurement method was developed to directly determine the mirror tilt/orientation using only one picture. The idea, that

well aligned mirrors share the same center of curvature and for a misaligned mirror the center of curvature differs from its ideal position, was adopted. The process to obtain the mirrors misalignments involves mainly image processing and digital photogrammetry techniques. The influence of the used optical system, pressure and temperature changes is considered in the calculations.

The information about the mirror alignment can be used in the reconstruction and analysis package for the RICH1 detector, called RICHONE. The corrections could be also applied directly to the mirrors if the mirror wall is equipped by remotely driven actuators.

The possibility to correct the mirror misalignments without accessing the radiator vessel has other advantages: If the vessel is always closed, the mirror segments can be constantly kept in a dry, clean atmosphere, thus preventing the degradation of the reflecting surface by moisture and dust. Measuring the mirrors misalignments and possibly adjusting their position can enhance the RICH1 performance by means of increase of the resolution of the measured Cherenkov angle and consequently by increase of the range of momentum for K/π separation.

It is convenient to emphasize that the method for absolute mirror misalignment measurements is new and it was fully developed in this Thesis. The method was properly tested and in the case of mirrors misalignments measurements its accuracy is comparable to the laser interferometry method. In comparison with the theodolite measurements, the CLAM method offers better measurement comfort, i.e. remote access measurements, higher speed of the procedure. The newly developed method can be used in other Cherenkov detectors as well.

Bibliography

[1] E. Albrecht *et al.*, "Status and characterisation of COMPASS RICH-1," *Nuclear Instruments and Methods in Physics Research Section A: Accelerators, Spectrometers, Detectors and Associated Equipment*, vol. 553, no. 12, pp. 215–219, Nov. 2005.

[2] S. Costa, "The mirror system of COMPASS RICH-1," INP Demokritos, 2002.

[3] "New compass page," http://wwwcompass.cern.ch/.

[4] A. Gorišek, P. Križan, S. Korpar, and M. Starič, "Alignment of the HERA-B RICH optical system with data," *Nuclear Instruments and Methods in Physics Research Section A: Accelerators, Spectrometers, Detectors and Associated Equipment*, vol. 433, no. 12, pp. 408–412, Aug. 1999.

[5] A. Papanestis, G. Vidal-Sitjes, P. Soler, and A. Macgregor, "Laser alignment monitoring system (LAMS) for the RICH," in *CERN Document Server*, vol. 2007, CERN, Geneve, Jun. 2007.

[6] J. C. Gayde, "COMPASS RICH - CLAM," technical report, CERN, Geneve, May 2007.

[7] S. Costa *et al.*, "CLAM, a continuous line alignment and monitoring method for RICH mirrors," *Nuclear Instruments and Methods in Physics Research Section A: Accelerators, Spectrometers, Detectors and Associated Equipment*, vol. 553, no. 12, pp. 135–139, Nov. 2005.

[8] "Philips lumileds LED lighting | LUXEON LEDs | LED lighting solutions," http://www.philipslumileds.com/.

[9] M. Svec, "Online monitoring mirrors in detector of cherenkov´s radiation," DIploma thesis, Technical Univezity of Liberec, Sep. 2007.

[10] "Refractive index tables," http://refractiveindex.info.

[11] E. Albrecht *et al.*, "The radiator gas and the gas system of COMPASS RICH-1," *Nuclear Instruments and Methods in Physics Research Section A: Accelerators, Spectrometers, Detectors and Associated Equipment*, vol. 502, no. 1, pp. 266–269, Apr. 2003.

[12] "Canon global," http://www.canon.com/.

[13] P. Abbon *et al.*, "Design and construction of the fast photon detection system for COMPASS RICH-1," *Nuclear Instruments and Methods in Physics Research Section A: Accelerators, Spectrometers, Detectors and Associated Equipment*, vol. 616, no. 1, pp. 21–37, Apr. 2010.

[14] COMSOL, "Comsol multiphysics user's guide, version 4.3a," Nov. 2012.

[15] "COMPASS RICH1," http://wwwcompass.cern.ch/compass/detector/..rich/welcome.html.

[16] J. B. MacQueen, "Some methods for classification and analysis of MultiVariate observations," in *Proc. of the fifth Berkeley Symposium on Mathematical Statistics and Probability*, L. M. L. Cam and J. Neyman, Eds., vol. 1. University of California Press, 1967, pp. 281–297.

[17] N. Otsu, "A threshold selection method from gray-level histograms," *IEEE Transactions on Systems, Man and Cybernetics*, vol. 9, no. 1, pp. 62–66, Jan. 1979.

[18] P. Dalloz and R. Valbuena, "THE COMPASS RICH-1 MIRROR WALL GEOMETRY," Tech. Rep. EST-ESI/99-08 Rev 2, 2000.

[19] P. Abbon *et al.*, "Particle identification with COMPASS RICH-1," *Nuclear Instruments and Methods in Physics Research Section A: Accelerators, Spectrometers, Detectors and Associated Equipment*, vol. 631, no. 1, pp. 26–39, Mar. 2011.

[20] S. Dalla Torre *et al.*, "Remote alignment of large mirror array for RICH detectors," *Nuclear Instruments and Methods in Physics Research Section A: Accelerators, Spectrometers, Detectors and Associated Equipment*, vol. 595, no. 1, pp. 220–223, Sep. 2008.

Publications of the Author

[1] L. Steiger, M. Šulc et al.: Monitoring of the absolute alignment of the COMPASS RICH-1 mirrors, submitted to *Nucl. Instrum. Methods Phys. Res.A*, February 2013.

[2] M. Šulc, J. Polák, L. Steiger, D. Kramer: Optická soustava pro detektor Čerenkovova záření. *JMO*, (2013) 52.

[3] L. Steiger, M. Šulc: Počítačová korekce rozladění polohy zrcadel v detektoru Čerenkovova záření RICH-1 experimentu COMPASS v CERN. *JMO*, (2013) 211-213.

[4] M. Šulc J. Polák, L. Steiger, D. Kramer, M. Finger, M. Slunečka: New optics for resolution improving of Ring Imaging Cherenkov detectors. *EPJ Web of Conferences* (2013) 48.

[5] M. Alexeev et al.: Mirror alignment control for COMPASS RICH-1 detector, *Nucl. Instrum. Methods Phys. Res.*, A 639 (2011), 219-221

[6] M. Šulc et al.: On-line mirror alignment monitoring method for COMPASS RICH-1, *Nucl. Instrum. Methods Phys. Res.*, A 595 (2008) 194-196.

[7] S. Levorato, et al.: Remote alignment of large mirror array for RICH detectors, *Nucl. Instr. and Meth.*, A 595 (2008) 220-223.